PERGAMON

Chemical Engineering Science 54 (1999) 2873–2881

Chemical Engineering Science

The influence of mass transfer and mixing on the performance of a tray column for reactive distillation

A.P. Higler[a,b], R. Taylor[a], R. Krishna[b,*]

[a] Department of Chemical Engineering, Clarkson University, Potsdam, NY 13699-5705, USA
[b] Department of Chemical Engineering, University of Amsterdam, Nieuwe Achtergracht 166, 1018 WV Amsterdam, The Netherlands

Abstract

We develop a generic steady-state design model for reactive distillation tray columns involving arbitrary liquid-phase reactions. The main features of this model are:

(1) The generalized Maxwell-Stefan diffusion equations are used to model the transfer in the vapour and liquid phases.
(2) The interphase energy transfer relations are properly taken into account.
(3) Chemical reactions taking place both in the diffusion "film" and bulk liquid phase are allowed.
(4) For description of the cross-flow of vapour and liquid phases at any given stage, a multi-cell modelling approach is adopted. By choosing the number of cells in the direction of the flow of the vapour and liquid phases, conditions of plug flow, well-mixed and intermediate mixing characteristics of either fluid phases can be realized,.
(5) Tray hydraulics and mass transfer relations are incorporated into the model and the program can be run in a true design mode, whereby the initial tray specification and layout using guess values of internal flows are updated using the actual flows as iterations proceed.

The usefulness of the developed nonequilibrium cell model is demonstrated by means of a case study involving hydration of ethylene oxide to ethylene glycol using kinetic data from the literature (Ciric and Miao, Ind. Engng. Chem. Res. 33, 2738–2748, 1994). We confirm the existence of multiple steady states, reported earlier by Ciric and Miao (1994) in a study using a model assuming that the vapour and liquid phases are in thermodynamic equilibrium. Introduction of interphase mass transfer resistance is seen to decrease the production of ethylene glycol and at the same time increases the formation of the by-product di-ethylene glycol. The formation of di-ethylene glycol is reduced when we increase the degree of staging in the liquid phase by increasing the number of well-mixed cells along the liquid flow path. This case study underlines the importance of tray hardware design on the reaction selectivity.

Keywords: Reactive distillation; Ethylene glycol; Maxwell–Stefan equations; Energy balance; Multiple steady states; Tray design

1. Introduction

Currently there is considerable academic and industrial interest in multi-functional reactors, involving in situ separation of products from the reactants (Krishna and Sie, 1994; Westerterp, 1992). Reactive distillation is one of the most common means of in situ product removal (Agreda et al., 1990; DeGarmo et al., 1992; Doherty and Buzad, 1992; Venkataraman et al., 1990). Both homogeneous and heterogeneous catalyzed chemical reactions can be carried out in a reactive distillation column (Sundmacher, 1995). There are three possible benefits of reactive distillation operation.

1. Higher conversions are obtained due to shifting of the equilibrium to the right. This is exemplified by the production of methyl acetate (Agreda et al., 1990; Siirola, 1995) and tert-amyl ether (Bravo et al., 1993).
2. Improved selectivity is obtained because of removal of products from the reaction zone. Such benefits are obtained for example in the production of propylene

* Corresponding author. Tel.: +31-20-525 7007; fax: +31-20-525 5604.
E-mail address: krishna@chemeng.chem.uva.nl. (R. Krishna)

0009-2509/99/$ – see front matter
PII: S0009-2509(98)00317-0

oxide from propylene chlorohydrins (Carra et al., 1979a, b) and in the alkylation of benzene to produce cumene (Shoemaker and Jones, 1987).

3. Benefits of heat integration are obtained because the heat generated in the chemical reactions are used for vaporization. This is particularly advantageous for situations involving high heats of reaction such as the hydration of ethylene oxide to ethylene glycol (Ciric and Gu, 1994).

A typical set-up used for reactive distillation is shown in Fig. 1. A column is usually split up into three sections: A reactive section, in which the reactants are converted into products and where, by means of distillation, the products are lifted (or flushed) out of the reactive zone. The tasks of the rectifying and stripping sections depend on the boiling points of reactants and products. If the product is the lowest boiling component in the process, the rectifying section is used for product purification and reactant recycle, and the stripping section mainly for inert and by-product removal as well as reactant recycle. In case the product is the highest boiling component, the tasks of the sections are switched.

If the reaction is heterogeneously catalyzed, the reactive zone is formed by a catalytic packing suitable for reactive distillation. In case of a homogeneously catalyzed reaction the reactive section is defined by the feed stream location of a homogeneous catalyst. If the catalyst can be considered to be non-volatile this means that the catalyst will only be found on and below the catalyst feed stage thus defining the reactive zone. With the set-up as shown in Fig. 1, it is possible to virtually eliminate an entire post-processing train in a process. One of the most spectacular examples of this kind is the Eastman process for production of methyl acetate (Siirola, 1995).

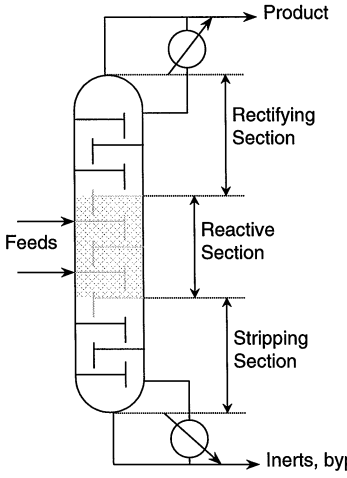

Fig. 1. Typical configuration of a reactive distillation tray column consisting of three sections: (a) rectifying section, (b) reactive section and (c) stripping section.

Within the reactive zone of a reactive distillation column a number of factors will determine the overall reaction rate and selectivity: these include (a) phase equilibrium, (b) interphase mass transfer, (c) chemical kinetics, (d) phase hold-ups and (e) residence time distributions (RTD) of the phases. Furthermore, there is interaction between these phenomena: the chemical reaction could influence mass transfer and the liquid RTD will influence the local reaction rates and selectivities. The interphase mass transfer, holdups and RTD of the phases are influenced by the design of the column, its internals and operating regime. For design purposes a variety of models is available in the literature.

First, we have steady-state models in which the vapour and liquid phase are assumed to be in equilibrium and allowance is made for finite reaction rates (Abufares and Douglas, 1995; Alejski et al., 1988; Carra et al., 1979; Ciric and Gu, 1994; Ciric and Miao, 1994; Eldarsi and Douglas, 1998; Jacobs and Krishna, 1993; Nijhuis et al., 1993; Pilavachi et al., 1997; Simandl and Svrcek, 1991; Venkataraman et al., 1990). Such models stem from conventional equilibrium-stage modelling of distillation columns. However, for reactive distillation the estimation of the height equivalent to a theoretical plate (HETP) or tray efficiencies for packed and tray columns is a much more difficult, if not an impossible task. This is because in the presence of chemical reactions the concept of tray efficiency is devoid of any physical meaning and can have positive, zero or negative values with almost no change in the hydrodynamic conditions (Higler et al., 1998).

In the second group of models, the column dynamic behaviour is taken into account while retaining the assumption of vapour–liquid-phase equilibrium and finite chemical kinetics (Abufares and Douglas, 1995; Espinoza et al., 1994; Ruiz et al., 1995; Scenna et al., 1998; Schrans et al., 1996).

The third group of models are the rate-based models for reactive distillation, which follow the philosophy of rate-based models for conventional distillation (Krishnamurthy and Taylor, 1985; Taylor and Krishna, 1993) and in some cases using rigorous Maxwell–Stefan theory for calculation of the interphase heat and mass transfer rates (Bravo et al., 1993; Higler et al., 1998; Kreul et al., 1998; Sawistowski and Pilavakis, 1979; Sundmacher, 1995; Sundmacher and Hoffmann, 1996; Zheng and Xu, 1992). However there is an important limitation in all of these published studies. This relates to the fact that the vapour and liquid phases are considered to be well-mixed on any stage. The assumption of a well-mixed liquid phase is a reasonable one for laboratory-scale equipment and commercial tray columns in which multiple downcomers are used. However, for large diameter tray columns with a single flow path, there would be considerable degree of staging of the liquid phase (Bennett and Grimm, 1991; Lockett, 1986), which can be expected to have an important effect on conversion and selectivity.

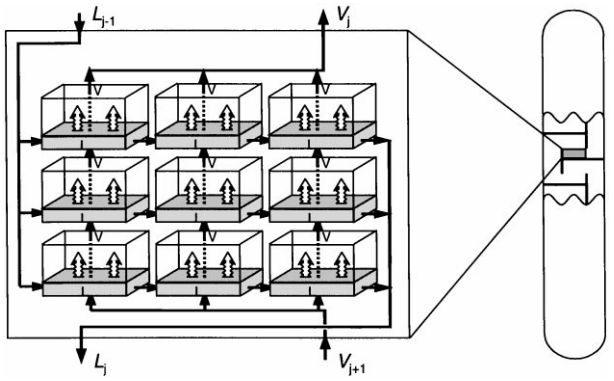

Fig. 2. Schematic diagram of the non-equilibrium cell model.

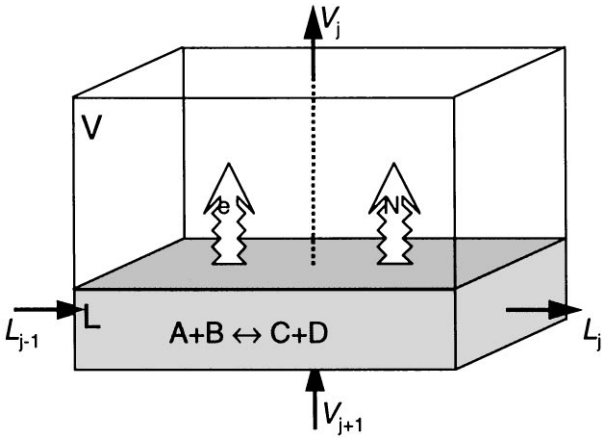

Fig. 3. Vapour–liquid contacting in a single non-equilibrium cell.

The major objective of this work is to develop a generic steady-state model for a reactive distillation tray column involving arbitrary homogeneous liquid-phase reactions. The distinguishing feature of the approach to be presented here is that on each stage in the column the true mixing characteristics of the vapour and liquid phases can be taken into account by appropriate choice of the number of well-mixed cells in the vapour and liquid flow direction; see Fig. 2. Furthermore, the model has been implemented in a true design mode, allowing the column hardware specifications to be determined. With the help of a case study for hydration of ethylene oxide to ethylene glycol, we highlight several features in the design of reactive distillation tray columns, not all of which have been recognized in the growing literature in this area. In particular, the hardware design aspects are highlighted.

2. Development of the non-equilibrium cell model

We first develop the model equations for the case in which each stage in the column is modelled as a single non-equilibrium cell, depicted in Fig. 3. The overall mole balance for the liquid phase can be written for this cell as

$$\mathrm{LMB} \equiv L_j - L_{j-1} - F_j^L \tilde{N}_{t,j}^L - \sum_{m=1}^{r} \sum_{i=1}^{n} v_{i,m} R_{m,j} \varepsilon = 0 \quad (1)$$

and the corresponding relation for the vapour phase is

$$\mathrm{VMB} \equiv V_j - V_{j+1} - F_j^V + \tilde{N}_{t,j}^V = 0. \quad (2)$$

Here L_j and V_j are the total molar liquid and vapour flow rates leaving stage j, F^L and F^V are the liquid and vapour molar feed rates, $\tilde{N}$ represents the interphase mass transfer rate, $v_{i,m}$ represents the stoichiometric factor for component i in reaction m, n denotes the number of components, $R_{m,j}$ is the reaction rate of reaction m at stage j, and ε is the total liquid volume in the contacting cell. Superscripts L and V indicate liquid and vapour phases. The individual component balance for the liquid phase is

$$\mathrm{LCB} \equiv L_j x_{i,j} - L_{j-1} x_{i,j-1} - f_{i,j}^L - \tilde{N}_{i,j} - \sum_{m=1}^{r} v_{i,m} R_{m,j} \varepsilon = 0 \quad (3)$$

with the corresponding relation for the vapour phase:

$$\mathrm{VCB} \equiv V_j y_{i,j} - V_{j+1} y_{i,j+1} - f_{i,j}^V + \tilde{N}_{i,j} = 0 \quad (4)$$

Here $x_{i,j}$ and $y_{i,j}$ are the liquid and vapour bulk mole fractions of component i at stage j, respectively. $f_{i,j}$ represents the total molar feed of component i to stage j.

The liquid-phase energy balance is given by

$$\mathrm{LEB} \equiv L_j H_j^L - L_{j-1} H_{j-1}^L - F_j^L H_j^{LF} - e_j^L + Q_j^L = 0. \quad (5)$$

For the vapour phase the corresponding relation is

$$\mathrm{VEB} \equiv V_j H_j^V - V_{j+1} H_{j+1}^V - F_j^V H_j^{VF} + e_j^V + Q_j^V = 0. \quad (6)$$

Here, e is the energy transfer rate from liquid to vapour phase, Q is a stage heat duty, which may be specified for both vapour and liquid phases. H^V and H^L are the vapour and liquid enthalpies, respectively. H^{VF} and H^{LF} are the vapour and liquid feed enthalpies.

2.1. Mass transfer

Vapour–liquid mass transfer will be described with the generalized Maxwell–Stefan theory (Krishna and Wesselingh, 1997; Taylor and Krishna, 1993). The underlying principle of the Maxwell–Stefan theory is that relative motion between diffusing species is balanced by friction. The driving force for species motion is the gradient of the chemical potential. This driving force is balanced by the friction between the moving molecules. For a system

of n components, there are $n-1$ independent Maxwell–Stefan equations. The concentration profile of the component n can be calculated from the summation equation. Fluxes are linked by a so-called bootstrap equation (Taylor and Krishna, 1993). In case of distillation, continuity of energy fluxes across the interface is the required bootstrap relation.

For the first $n-1$ components we have the following Maxwell–Stefan equations:

$$\frac{x_{i,j}}{\mathbb{R}T}\left(\frac{\partial \mu_i}{\partial \eta}\right)_j \equiv d_{i,j} = \sum_{l=1}^{n} \frac{x_{i,j}\tilde{N}_{l,j} - x_{l,j}\tilde{N}_{i,j}}{c_t^L \kappa_{i,l}^L a}. \tag{7}$$

Here η is the dimensionless distance coordinate in the "film", a is the total vapour–liquid interfacial area on stage j, and $\kappa_{i,j}$ is the binary mass transfer coefficient. Since only $n-1$ of the MS equations are independent, the compositions of the nth component can be obtained from the summation equation

$$\sum_{i=1}^{n} x_{i,j} = 1. \tag{8}$$

In a reactive system, we have to take into account the reaction in the transfer film as well; the reaction will create or remove a species, thereby altering the component flux. We can therefore write

$$\left(\frac{\partial \tilde{N}_{i,j}}{\partial \eta}\right) = a\delta^L \sum_{m=1}^{\mathrm{r}} \nu_{i,m} R_{m,j}, \tag{9}$$

where δ^L is the liquid-phase mass transfer film thickness.

The fluxes are linked together at the interface by a "bootstrap" equation; here we require that the energy flux be continuous across the vapour–liquid interface,

$$e_j^V = e_j^L, \tag{10}$$

where

$$e_j^V = -\frac{a\lambda^V Le^V}{\delta^V}\left(\frac{\partial T}{\partial \eta}\right) + \sum_{i=1}^{n} \tilde{N}_{i,j} H_i^V \tag{11}$$

and

$$e_j^L = -\frac{a\lambda^L Le^L}{\delta^L}\left(\frac{\partial T}{\partial \eta}\right) + \sum_{i=1}^{n} \tilde{N}_{i,j} H_i^L. \tag{12}$$

Here Le is the Lewis number, which is defined as the film thickness for mass transfer divided by the film thickness for heat transfer, λ is the mixture thermal conductivity. The temperature profiles in the vapour and liquid phases are determined by the fact that the energy fluxes also be continuous within the respective diffusion films, i.e.

$$\frac{\partial e_j^L}{\partial \eta} = \frac{\partial e_j^V}{\partial \eta} = 0. \tag{13}$$

For the liquid film we therefore get

$$-a\lambda^L\left(\frac{Le^L}{\delta^L}\right)^2\left(\frac{\partial^2 T}{\partial \eta^2}\right) + \frac{1}{\delta^L}\sum_{i=1}^{n}\left(H_i^L \frac{\partial \tilde{N}_{i,j}}{\partial \eta}\right) + \frac{1}{\delta^L}\sum_{i=1}^{n}\left(\tilde{N}_{i,j}\frac{\partial H_i^L}{\partial \eta}\right) = 0. \tag{14}$$

The first term of this equation is the change in conductive heat flux due to a temperature gradient. The second term represents the reaction enthalpy, and the third term represents the contributions of changes in enthalpies over the liquid film, originating from a temperature profile over the film ($H = H_0 + C_p \Delta T$) and from differences in excess enthalpy because of concentration gradients in the film.

2.2. Interface conditions

At the interface, we assume thermodynamic equilibrium; this implies

$$y_{i,j}^I = K_{i,j}^P x_{i,j}^I \tag{15}$$

and

$$T^{IL} = T^{IV}. \tag{16}$$

Here $K_{i,j}^P$ is the vapour–liquid equilibrium constant of component i on stage j. This vapour–liquid equilibrium constant is assumed to be a function of temperature, pressure and compositions of the vapour and liquid at the interface.

The resulting model described by Eqs. (1)–(16) represent a set of highly nonlinear, linked differential and algebraic equations. This system cannot be solved analytically, and we will therefore have to perform a finite difference approximation of the differential equations. Both vapour and liquid mass transfer "films" are divided into a number of grid points. The resulting finite difference equations, along with mole and energy balances form a system of nonlinear algebraic equations that can be solved numerically. We use Newton's method for this purpose.

2.3. Retrofit and design modes

Important factors in the description of mass transfer and reaction are the hydrodynamic and mass transfer parameters such as interfacial area a, liquid hold-up, ε, and mass transfer coefficient $\kappa_{i,j}$. These parameters depend directly on the physical properties of the system, the column hardware design (column diameter, choice of internals, design of internals) and the operating conditions. We have incorporated two different calculation modes to the modelling exercise. In the retrofit mode, the user specifies the details of the column internals and

design in advance of solving the set of equations. This mode is useful when simulating an existing column and our interest would be to determine the column performance. For grass-roots design of a reactive distillation tray column, the column diameter, tray design and layout are themselves unknown. For this purpose our program can also be run in a true design mode. We generate an initial tray layout, based on an initial guess of the internal flows and a design specification (e.g. operation at a specified fraction of flooding limit). The generated initial layout is used for calculation of the hydrodynamic parameters. With these hydrodynamic parameters, the improved estimates for process variables are calculated. Based on these new guesses, the trays are re-rated and checked if the operation regime falls within acceptable limits for operation (weeping, flooding, excessive entrainment). If this is not the case, the old design is discarded, and a new design is made. Otherwise the old design is retained. The tray design procedure used in this work is described in detail elsewhere (Kooijman, 1995; Kooijman and Taylor, 1995; Taylor et al., 1994). An important advantage of this method is that if the model converges, a consistent design will be obtained along with consistent results for the process variables. The disadvantage of the design approach is that there may be considerable difficulties in achieving convergence because design correlations (for flooding, hold-ups, clear liquid heights, etc.) are called up during every iteration. During iterations the operating conditions may be such that they go beyond the operable limits of the tray. This could cause the program to crash. User intervention for restarting the iterations with improved guesses of the flows, etc., is required in such cases.

2.4. Mixing

The biggest problem left untouched so far is that of liquid and vapour mixing behaviour on a stage. The residence times and residence time distributions of the liquid and vapour phase can severely affect the performance of a reactor. Modelling the mixing characteristics of the vapour and liquid phases is no simple matter. On a distillation tray there are several possible regimes of operation (Lockett, 1986; Zuiderweg, 1982) and each regime has its distinctive characteristics. Here we have adopted the multiple-cells-per-stage approach; see Fig. 2. The vapour–liquid dispersion on a tray is split up into several cells within which interphase mass transfer and subsequent chemical reactions occur. For each of these cells we can write a set of equations as presented above for a single cell. Various forms of mixing behaviour can now be modelled by specifying the number of cells in the direction of flow of the vapour and liquid phases. Literature correlations are available to determine these mixing characteristics (Bennett and Grimm, 1991; Fair et al., 1997).

By varying the number of cells in a flow path we can go from a perfectly mixed phase on a stage (one cell per flow path), to an approximation of plug flow (large number of cells, typically more than four). There is also the possibility of interconnecting the cells in different ways to represent say by-passing and channelling. To make the multi-cell model complete, we need to specify the interchange of liquid (with a molar flow rate of L_M) between horizontal rows of cells. In setting up the proper component and enthalpy balances for the multi-cell model we need to take the following considerations into account:

- The amount of liquid entering a cell from the cell above (below) is exactly the same as the amount of liquid leaving the cell to the cell below (above).
- The liquid mixing flow L_M is large as compared to the liquid cell flow.

With the above considerations, only the component (Eq. (3)) and energy balances (Eq. (5)) need to be modified. The component balance equation (3) is modified to

$$\mathrm{LCB} + L_M(2x_{i,j} - x_{i,j,\downarrow} - x_{i,j,\uparrow}) = 0. \tag{17}$$

Similarly, the energy balance equation (5) is modified as

$$\mathrm{LEB} + L_M(2H^L_j - H^L_{j,\downarrow} - H^L_{j,\uparrow}) = 0. \tag{18}$$

Here L_M is the vertical liquid mixing flow, $x_{i,j,\downarrow}$ and $x_{i,j,\uparrow}$ are the liquid-phase compositions of the cells above and below the cell under consideration. A similar nomenclature holds for the enthalpies. In practice, the vapour jet issuing from the holes on a tray will create a "fountain" effect; this will tend to mix the liquid phase more or less completely in the vertical direction (Lockett, 1986; Zuiderweg, 1982). In order to model this situation in which the liquid compositions in any vertical column of cells have the same composition, $x_{i,j} \approx x_{i,j,\downarrow} \approx x_{i,j,\uparrow}$, we choose a value of L_M which is considerably larger, say 10 times, than the liquid flow on that stage. In all the calculations presented below, the liquid phase in a vertical column of cells is assumed to be well mixed.

3. Case study: ethylene glycol

We will illustrate the features of the nonequilibrium cell model by means of a case study for production of ethylene glycol (EG) from ethylene oxide (EO) and water. Ethylene glycol is formed in an irreversible reaction from ethylene oxide and water:

$$\mathrm{EtO} + \mathrm{H_2O} \rightarrow \mathrm{EG}. \tag{19}$$

In addition, we have an unwanted consecutive reaction in which ethylene glycol reacts with ethylene oxide to di-ethylene-glycol (DEG):

$$\mathrm{EtO} + \mathrm{EG} \rightarrow \mathrm{DEG}. \tag{20}$$

The reaction rate constant of the second reaction is, under reaction conditions, about thrice as large as the rate constant of the first reaction. Therefore, in a conventional reactor with equimolar feed, a considerable amount of DEG is produced. Furthermore, the reactions are both highly exothermic requiring good temperature control. The classical strategy to tackle this selectivity problem is to use a high surplus of water in the reactor and operate the reactor at low conversion. In this manner the concentration of both ethylene oxide and ethylene glycol are kept relatively low, suppressing the rate of the unwanted second reaction. This, however, requires an extra separation unit to separate the product from the reactor exit stream and to recycle the unused reactants.

A good alternative for this conventional process is offered by reactive distillation. Here product formation, product separation and reactant recycle can be integrated in one piece of equipment. The big advantage of using reactive distillation in this case is that it combines the preferred reaction conditions with direct heat integration. By choosing the right operation conditions one can ensure that the column is largely filled with water. The ethylene oxide that is supplied to the column reacts almost instantly to EG and because of the high surplus of water, the concentrations of ethylene oxide and ethylene glycol will be very low. This results in a low production rate of DEG. Furthermore, the distillation process provides direct temperature control, since the temperature of the liquid phases will always be at boiling point. Hot spot formation and, therefore, the danger of runaway reactions is non-existent in reactive distillation.

Ciric and Gu (1994) proposed a 10-stage column for production of ethylene glycol. Water is supplied to the top of the column, while the ethylene oxide feed is distributed along the top section of the column. The reaction is assumed to take place only on the top five stages of the column. The column is operated at infinite reflux ratio, while in the bottom a boilup ratio of approximately 23 is maintained. Ciric and Miao (1994) used a homotopy continuation method to prove the existence of multiple steady states in the proposed set-up. In both these studies an equilibrium stage approach was used. In our case we have used a similar set-up to that of Ciric and Miao (1994), details of which are given in Fig. 4. In our calculations the nonequilibrium cell model was used for description of stages 2–9. The reaction kinetics and thermodynamics data are the same as those reported in the papers by Ciric et al. The condensor (stage 1) and the reboiler (stage 10) are modelled as equilibrium stages. Reactions are assumed to take place only on stages 2–6. Several calculations were carried out by varying the number of cells in the vapour and liquid flow directions. The calculation results for the nonequilibrium cell model will be denoted by NEQ (n_L, n_V) where the numbers n_L and n_V refer to the number of mixing cells in the liquid and vapour phases, respectively. To compare our results with those of Ciric and Miao (1994), we also performed calculations in which phase equilibrium was "forced" on all the stages by using extremely high values of the interphase transfer coefficients of heat and mass (obtained by multiplying the estimated values of the transfer coefficients by a factor of 10^5); such model calculation results are denoted by EQ.

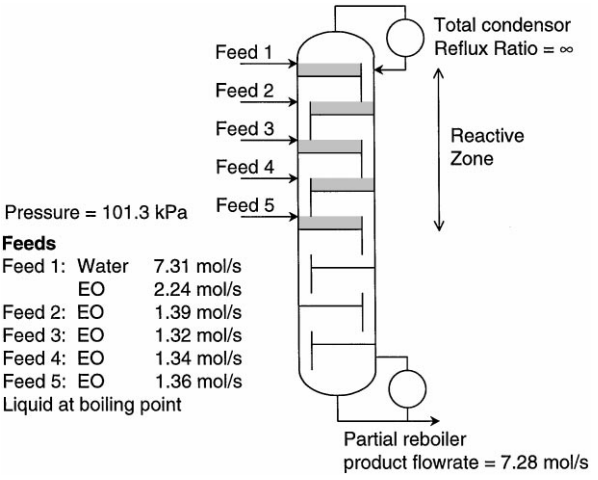

Fig. 4. Configuration of reactive distillation column for hydration of ethylene oxide to ethylene glycol. Further details to be found in Ciric and Miao (1994).

3.1. Multiple steady states

Both EQ and NEQ (1, 1) model calculation results yielded three steady-state solutions: high conversion steady-state, SS-1, low conversion state, SS-3, and the intermediate state, SS-2. The temperature profiles for these models are shown in Fig. 5. The EQ model calculations match those obtained by Ciric and Miao (1994). For the low conversion steady-state, SS-3, there is hardly any difference in the temperature profiles of the NEQ (1, 1) and EQ models. This is to be expected because there is hardly any reaction taking place in the column. For the other states, SS-1 and SS-2, there is a considerable difference in the temperatures in the bottom section, emphasizing the strong influence on interphase transfer resistances. The reason for this strong influence becomes clear when we compare the composition profiles for SS-1 using the EQ and NEQ (1, 1) models; see Fig. 6. There is a significant difference in the composition profiles in the bottom section. Due to the influence of interphase mass transfer it is more difficult to strip water from the liquid phase in the bottom section. The lower EG liquid compositions obtained in the bottom section in the NEQ (1, 1) model leads to significantly lower temperatures.

Fig. 7 presents a comparison of the vapour and liquid molar flows in the column for the three steady-state

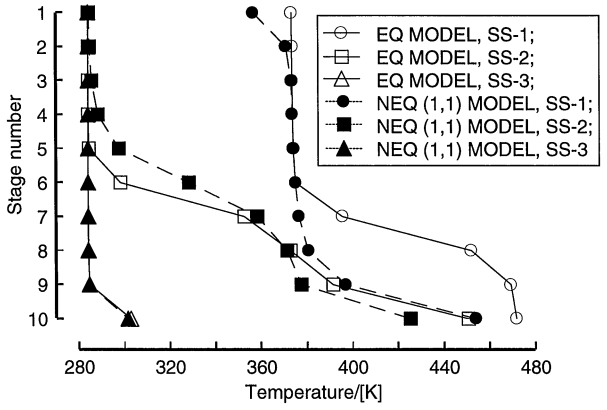

Fig. 5. Column temperature profiles for the three steady-state solutions using the EQ and NEQ (1, 1) models.

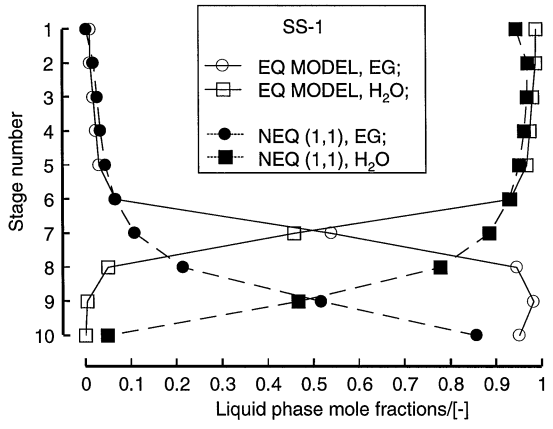

Fig. 6. Column composition profiles for the high conversion steady state SS-1 using the EQ and NEQ (1, 1) models.

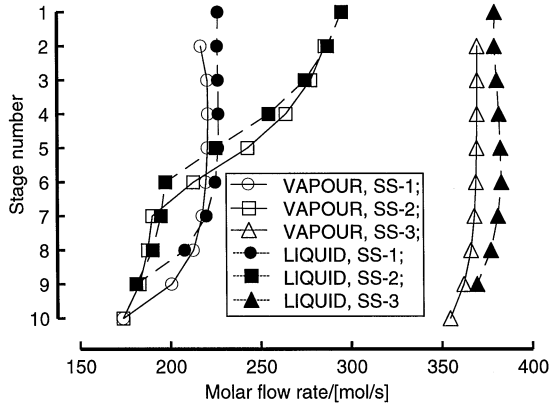

Fig. 7. Column molar flow profiles of the liquid and vapour phases for the three steady-state solutions using the NEQ (1, 1) model.

solutions obtained with the NEQ (1, 1) models. It is interesting to note that the low conversion steady-state SS-3 has the highest vapour–liquid traffic inside the column. A further point to note is that in SS-1 and SS-2

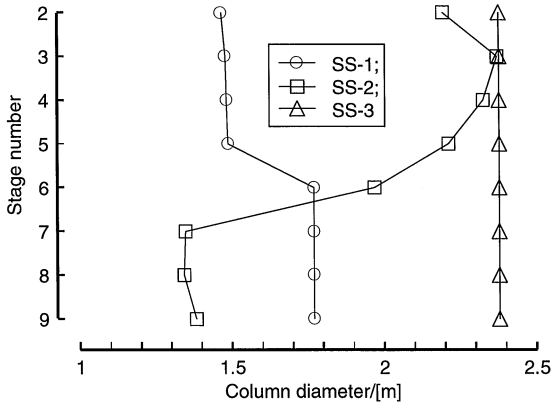

Fig. 8. Column diameters calculated for each stage assuming 75% flooding factors for the three steady-state solutions using the NEQ (1, 1) model.

there is a considerable difference in the molar flows in the top (reactive) and the bottom (stripping) sections. The differences in the molar flows in the top and bottom sections are due to the considerable differences in the molar heats of vaporization of the four species present in the mixture. Relative to that of water, the heats of vaporization are EO = 0.7, EG = 1.3 and DEG = 1.5. For SS-1, for example, the concentration of EO in the bottom section is practically zero and the mixture contains EG, DEG and water, all of which have a high heat of vaporization. It should also be clear that the commonly used assumption of equimolar overflow in conventional distillation is not valid for the reactive distillation study under consideration. The necessity of using a proper energy balance at the interface (Taylor and Krishna, 1993), as used in this study, is underlined.

Using the sieve tray sizing algorithm as outlined by Kooijman (1995) we can calculate the column diameters assuming 75% of the flooding limit for each stage; the column diameter calculations are shown in Fig. 8. We note that for SS-3 the column diameter is 2.4 m for all stages, whereas the high-conversion steady state solution demands 1.5 m column diameter in the reactive section and 1.8 m diameter in the stripping (non-reactive) section. The important conclusion to be drawn from the results of Figs. 7 and 8 is that if a column of an average diameter of say 1.6 m is built for the production of EG, it would be impossible to realize the states SS-2 and SS-3 because the column would be inoperable due to flooding of some (in case SS-2) or all (in the SS-3 case) of the trays. Put in another way, for a chosen column hardware design, only one steady-state solution is achievable in the column. In the literature on reactive distillation, considerable attention has been paid to the phenomena of multiple steady states (Eldarsi and Douglas, 1998; Jacobs and Krishna, 1993; Nijhuis et al., 1993; Hauan et al., 1995). However, in all these models, no attention has been paid to the column design aspects and the influence

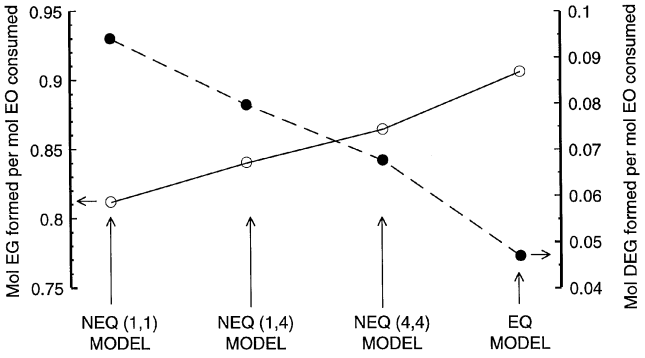

Fig. 9. Selectivity towards production of EG and DEG for the high conversion steady state using NEQ (1, 1), NEQ (1, 4), NEQ (4, 4) and EQ models.

of vapour–liquid traffic thereon. The case study above has emphasized the importance of column design on the realizability, or otherwise, of multiple steady states.

3.2. *Influence of mass transfer and mixing on selectivity*

Applying chemical reaction engineering principles we should expect that the selectivity to EG should improve with improved mass transfer and with increased staging in the vapour and liquid phases. To demonstrate this aspect we compare the selectivities for SS-1 obtained with NEQ (1, 1), NEQ (1, 4), NEQ (4, 4) and EQ models; see Fig. 9. The best selectivity is obtained with the EQ model. Increasing the number of non-equilibrium cells in the vapour phase improves mass transfer performance and therefore conversion of EO. Increasing the number of well-mixed stages in the liquid phase has a beneficial effect both on interphase mass transfer and on the reaction selectivity. From a hardware design viewpoint it is preferable to choose a tray design with a long liquid flow path, which will ensure sufficient staging in the liquid phase.

4. Conclusions

We have developed a non-equilibrium cell model for the design of reactive distillation tray columns. By appropriate choice of the number of cells in the vapour and liquid flow directions the mass transfer and mixing characteristics of real trays can be simulated. Using the case study of the hydration of ethylene oxide to ethylene glycol we have highlighted some essential features of reactive distillation columns involving homogeneous liquid-phase reactions. Interphase mass and energy transfer resistances have a significant effect on the formation of the by-product di-ethylene glycol. Staging in the vapour and liquid phases also influences reaction selectivity to EG. While multiple steady states are possible using both NEQ and EQ models, it is possible that not all steady states would be realizable in practice due to flooding phenomena. This underlines the importance of simultaneously considering hardware design along with process aspects.

Notation

a	vapour liquid interfacial area, m^2
c_t	total concentration, mol/m^3
C_p	molar heat capacity, J/mol K
d	driving force for mass transfer, dimensionless
e	energy transfer rate, J/s
f	molar feed rate of a component, mol/s
F	molar feed rate, mol/s
H	molar enthalpy, J/mol
K^P	phase equilibrium constant, dimensionless
L	liquid molar flowrate, mol/s
LCB	liquid component balance, defined in Eq. (3), mol/s
Le	Lewis number, dimensionless
LEB	liquid energy balance, defined in Eq. (5), J/s
LMB	total liquid mole balance, defined in Eq. (1), mol/s
n	total number of components,
$\tilde{N}$	interphase mass transfer rate, mol/s
Q	heat duty, J/s
r	total number of reactions, dimensionless
$\mathbb{R}$	gas constant, 8.314 J/mol K
R	reaction rate, mol/m^3 s
T	temperature, K
V	vapour molar flow rate, mol/s
VCB	vapour component balance, defined in Eq. (4), mol/s
VEB	vapour energy balance, defined in Eq. (6), J/s
VMB	total vapour mole balance, defined in Eq. (2), mol/s
x	mole fraction liquid-phase component, dimensionless
y	mole fraction vapour-phase component, dimensionless
z	distance coordinate with diffusion "film", m

Greek letters

δ	film thickness, m
Δ	difference, dimensionless
ε	liquid volume in a contacting cell, m^3
η	dimensionless coordinate in the diffusion film $= z/\delta$,
κ	mass transfer coefficient, m/s
λ	thermal conductivity, W/m K
μ	chemical potential, J/mol
ν	stoichiometric coefficient for reaction, dimensionless

Subscripts

i	index indicating component number
j	index indicating stage number
l	summation index for components
M	mixing stream in cell model
m	index indicating reaction number
t	summation over all components
$\uparrow$	cell above the cell under consideration
$\downarrow$	cell beneath the cell under consideration

Superscripts

F	feed
I	interface
L	liquid-phase
V	vapour-phase

References

Abufares, A.A., and Douglas, P.L. (1995). Mathematical modeling and simulation of an MTBE catalytic distillation process using SPEEDUP and AspenPlus. *Trans I Chem. E*., *73* (part A), 3–12.

Agreda, V.H., Partin, L.R., & Heise, W.H. (1990). High-purity methyl acetate via reactive distillation, *Chem. Engng Prog*., *2*, 40–46.

Alejski, K., Szymanowski, J., & Bogacki, M. (1988). The application of a minimization method for solving reactive distillation problems. *Comput. Chem. Engng*, *12*, 833–839.

Bennett, D.L., & Grimm, H.J. (1991). Eddy diffusivity for distillation sieve trays. *A.I.Ch.E. J*., *37*, 589–596.

Bravo, J.L., Pyhalathi, A., & Jaervelin, H. (1993). Investigations in a catalytic distillation pilot plant: Vapour/liquid equilibrium, kinetics and mass transfer issues. *Ind. Engng Chem. Res*., *32*, 2220–2225.

Carra, S., Morbidelli, M., Santacesaria, E., & Buzzi, G. (1979b). Synthesis of propylene oxide from propylene chlorohydrins – II. Modeling of the distillation with chemical reaction unit. *Chem. Engng Sci*., *34*, 1133–1140.

Carra, S., Santacesaria, E., Morbidelli, M., Cavalli, L., (1979a). Synthesis of propylene oxide from propylene-chlorohydrins – I: Kinetic aspects of the process. *Chem. Engng Sci*., *34*, 1123–1132.

Ciric, A.R., & Miao, P. (1994). Steady state multiplicities in an ethylene glycol reactive distillation column. 1994, *Ind. Engng Chem. Res*., *33*, 2738–2748.

Ciric, A.R., & Gu, D., (1994). Synthesis of nonequilibrium reactive distillation by MINLP optimization, *A.I.Ch.E. J*., *40*, 1479–1487.

DeGarmo, J.L., Parulekar, V.N., & Pinjala, V., (1992). Consider reactive distillation. *Chem. Engng Prog*., *3*, 43–50.

Doherty, M.F., & Buzad, G., (1992). Reactive distillation by design. *Trans I. Chem. E*., Part A, *70*, 448–458.

Eldarsi, H.S., & Douglas, P.L. (1998). Methyl-tert-butyl ether catalytic distillation column. Part I: Multiple steady states. *Trans. I. Chem. E*., Part A, *76*, 509–516.

Espinoza, J., Martinez, E., & Perez, G.A. (1994). Dynamic behavior of reactive distillation columns, Equilibrium systems. *Chem. Engng Commun*., *128*, 19–42.

Fair, J.R., Steinmeyer, D.E., Penney, W.R., & Croker, B.B. (1997). Gas absorption and gas–liquid system design. In D.W. Green, & J.O. Maloney (Eds.), *Perry's chemical engineers' handbook*, (7th Edition, Section 14). New York: McGraw-Hill.

Hauan, S., Hertzberg, T., & Lien, K.M. (1995). Why methyl-*tert*-butyl-ether production by reactive distillation may yield multiple solutions. *Ind. Engng Chem. Res*., *34*, 987–991.

Higler, A.P., Taylor, R., & Krishna, R. (1998). Modeling of a reactive separation process using a nonequilibrium stage model. *Comput. Chem. Engng*, *22* (Suppl.) S111–S118.

Jacobs, R., & Krishna, R. (1993). Multiple solutions in reactive distillation for methyl-*tert*-butyl ether synthesis. *Ind. Engng Chem. Res*., *32*, 1706–1709.

Kooijman, H.A. (1995). *Dynamic nonequilibrium column simulation*. Ph.D. dissertation, Clarkson University, Potsdam, USA.

Kooijman, H.A., & Taylor, R. (1995). Nonequilibrium model for dynamic simulation of tray distillation columns. *A.I.Ch.E. J*., *41*, 1852–1863.

Kreul, L.U., Gorak, A., Dittrich, C., & Barton, P.I. (1998). Dynamic catalytic distillation: Advanced simulation and experimental validation, *Comput. Chem. Engng*, *22,* S371–S378.

Krishna, R., & Sie, S.T. (1994). Strategies for multiphase reactor selection. *Chem. Engng Sci*., *49*, 4029–4065.

Krishna, R., & Wesselingh, J.A. (1997). The Maxwell–Stefan approach to mass transfer. *Chem. Engng Sci*., *52*, 861–911.

Krishnamurthy, R., & Taylor, R. (1985). Nonequilibrium stage model of multicomponent separation processes, *A.I.Ch.E. J*., *32*, 449–465.

Lockett, M.J. (1986). *Distillation tray fundamentals*. Cambridge: Cambridge University Press.

Nijhuis, S.A., Kerkhof, F.P.J.M., & Mak, A.N.S. (1993). Multiple steady states during reactive distillation of methyl-*tert*-butyl ether. *Ind. Engng Chem. Res*., *32*, 2767–2774.

Pilavachi, P.A., Schenk, M., Perez-Cisneros, E., & Gani, R. (1997). Modeling and simulation of reactive distillation operations, *Ind. Engng Chem. Res*., *36*, 3188–3197.

Ruiz, C.A., Basualdo, M.S., & Scenna, N.J. (1995). Reactive distillation dynamic simulation. *Trans. I. Chem. E*. Part A, *73*, 363–378.

Sawistowski, H., & Pilavakis, P.A., (1979). Distillation with chemical reaction in a packed column. *I. Chem. E Symp Ser*., *no. 56*, 49–63.

Scenna, N.J., Ruiz, C.A., & Benz, S.J. (1998). Dynamic simulation of startup procedures of reactive distillation columns. *Comput. Chem. Engng*., *22,* S719–S722.

Schrans, S., de Wolf, S., & Baur, R. (1996). Dynamic simulation of reactive distillation. An MTBE case study. *Comput. Chem. Engng*, *20* (Suppl.), S1619–S1624.

Shoemaker, J.D., & Jones, E.M., (1987). Cumene by catalytic distillation. *Hydrocarbon Processing*, 57–58.

Siirola, J.J. (1995). An industrial perspective on process synthesis. *A.I.Ch.E. Symp. Ser. No.* 304, *91*, 222–233.

Simandl, J., & Svrcek, W.Y. (1991). Extension of the simultaneous solution and inside-outside algorithms to distillation with chemical reactions. *Comput. Chem Engng*, *15*, 337–348.

Sundmacher, K. (1995). *Reaktivdestillation mit katalytischen Fuellkoerperkackungen – ein neuer Process zur Herstellung der Kraftstoffkomponente MTBE*. Ph.D thesis, ISBN 3-930697-86-6.

Sundmacher, K. & Hoffmann, U. (1996). Development of a new catalytic distillation process for fuel ethers via a detailed nonequilibrium model. *Chem. Engng Sci*., *51*, 2359–2369

Taylor, R., Kooijman, H.A., & Hung, J.-S. (1994). A second generation nonequilibrium model for computer simulation of multicomponent separation processes. *Comput. Chem Engng*, *18*, 205–217.

Taylor, R. & Krishna, R. (1993). *Multicomponent mass transfer*. New York: Wiley.

Venkataraman S., Chan, W.K., & Boston, J.F. (1990). Reactive distillation using ASPEN PLUS. *Chem. Engng Prog*., *86*(8), 45–54.

Westerterp, K.R. (1990). Multifunctional reactors. *Chem. Engng Sci*., *9–11*, 2195–2206.

Zheng Y., & Xu, X. (1992). Study on catalytic distillation processes, Part II: Simulation of catalytic distillation processes, Quasi homogeneous and rate based model. *Trans. I. Chem. E*., Part A, *70*, 465–470.

Zuiderweg, F.J. (1982). Sieve trays – A view on the state of art. *Chem. Engng Sci*., *37*, 1441–1461.